

# Molecular design of calcimycin (A23187) evidenced by the complexing behaviour of its 4-bromo and 19-demethyl analogues

Stéphane Vila,<sup>a</sup> Isabelle Canet,<sup>\*a</sup> Jacques Guyot,<sup>a</sup> Georges Jeminet<sup>\*a</sup> and Yvon Pointud<sup>b</sup>

<sup>a</sup> Laboratoire de Synthèse et Etude de Systèmes à Intérêt Biologique (CNRS UMR 6504), Université Blaise Pascal Clermont-Ferrand, Campus des Cézeaux, 63177, Aubière cedex, France. E-mail: isabelle.canet@chimie.univ-bpclermont.fr; Fax: +33 4 73 40 77 17

<sup>b</sup> Laboratoire de Thermodynamique des Solutions et des Polymères (CNRS UMR 6003), Université Blaise Pascal Clermont-Ferrand, Campus des Cézeaux, 63177, Aubière cedex, France

Received (in Montpellier, France) 9th January 2003, Accepted 18th March 2003

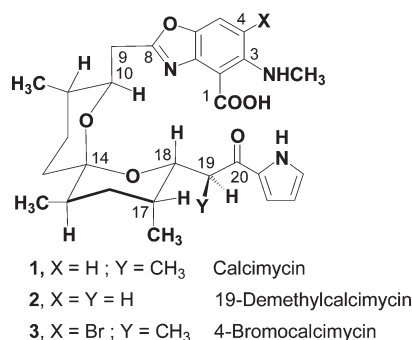
First published as an Advance Article on the web 2nd July 2003

An original comparison of the complexing properties of calcimycin (A23187) and its 4-bromo and 19-demethyl analogues with the alkaline earth cations,  $Mn^{2+}$  and  $Zn^{2+}$ , gives new insight on the molecular design of this universally used calcium ionophore.

Calcimycin or A23187<sup>1</sup> (**1** in Scheme 1), a bacterial metabolite belonging to the carboxylic polyether antibiotics group, is still attracting considerable attention in biology as a tool for the study of the calcium second messenger in living systems<sup>2</sup> owing to its calcium carrier properties.

We recently described for the first time a general way to modify the ketopyrrole arm of its skeleton by hemisynthesis, which enabled us to synthesise 19-demethylcalcimycin, **2**.<sup>3</sup> Also, in the course of our study of crystalline adducts of the 4-bromo derivative **3** (Scheme 1) with various divalent cations, we recently described the crystal structure obtained for  $Zn^{2+}$  with an unusual ligand arrangement.<sup>4</sup>

In the neutral complexes of calcimycin with divalent cations, which are the trans-membrane transporting species,<sup>5</sup> the benzoxazole moiety supplies two coordinating sites (O-carboxylate and N-oxazole), and the ketopyrrole one (O-ketone).<sup>6,7</sup> Here, by molecular modelling of **2**, and from solid state studies on **3**, we show that the structural modifications carried out at C19 and C4 induce local conformational changes in the liganding arms. Repercussions on the stability of complexes are then assessed by determining the thermodynamic equilibrium constants for the alkaline earth cations  $Zn^{2+}$  and  $Mn^{2+}$ . Potentiometry in pure methanol (25°C) proved suitable for this purpose. Molecular properties of calcimycin are deduced from the results.



Scheme 1

## Results and discussions

### Structural modifications

**19(S)-Methyl removal.** We were interested in the mobility of the ketopyrrole arm governed by interactions in the C17–C18–C19–C20 part of the molecule, with or without a 19(S)-Me group. We carried out calculations using the MacroModel<sup>®</sup> Program, with a Monte Carlo conformational search for the minimum energy, on a selected model in which the benzoxazole arm was replaced by a methyl group in the 10*eq* position (Fig. 1, structures I and II). In the calculations the conjugated ketopyrrole part was kept coplanar, and from the crystallographic data,<sup>6,7</sup> the spiroketal moiety was assumed to be undistorted.

Plots of relative energy *versus* variation in the dihedral angle C17–C18–C19–C20 are shown in Fig. 2, for a complete rotation around the C18–C19 bond. Two significant minima corresponding to conformers A and B were observed for model I, separated by a high rotational barrier. A non-significant minimum C was also noted. Conformer A is closely similar to that described for this part of the molecule in the structural results cited for calcimycin.<sup>6–8</sup> For model II, the curve was modified with a less stable A conformer and a significantly lowered rotational barrier between conformers A and B.

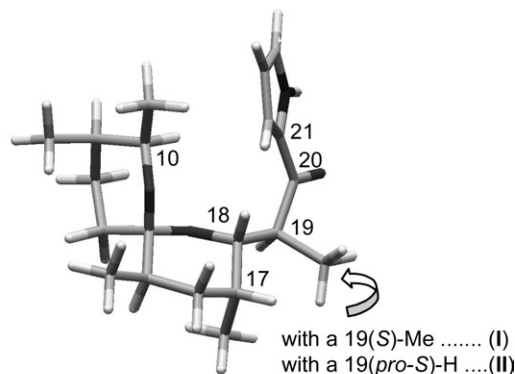


Fig. 1 Models I and II used for conformational calculations.

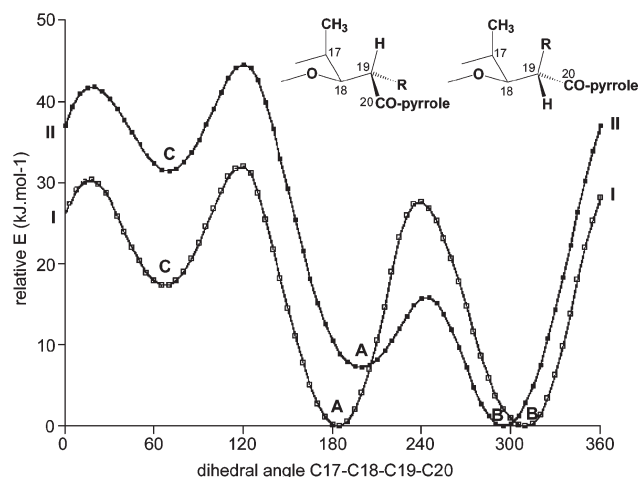


Fig. 2 Relative energy curves for models I and II.

Ramachandran plots including the C17–C18–C19–C20 and C18–C19–C20–C21 dihedral angles showed three potential wells for I (Fig. 3) corresponding to the previous conformers A, B and C. Large differences were still observed in the contour lines for II towards indefinite minima.

Does this modification of conformational mobility, with or without a 19(*S*)-methyl group, perturb the molecule's divalent cations recognition properties? We addressed this question by using demethylcalcimycin **2**.

**4-Bromo substitution.** A straightforward preparation of 4-bromocalcimycin (**3**) has been described,<sup>9</sup> subsequent to calcimycin isolation. Owing to its modified fluorescence spectrum compared with the natural metabolite, it has been proposed and marketed as a calcium ionophore for biological experiments, suitable for use in the presence of fluorescent probes.<sup>10</sup> More recently, Erdahl *et al.*<sup>11</sup> showed that **3** in fact transports  $\text{Zn}^{2+}$  and  $\text{Mn}^{2+}$  with high selectivity over  $\text{Ca}^{2+}$  in phospholipid vesicles. However, there was no information on either the thermodynamic equilibrium constants in solution for divalent cations, or the structure of cationic complexes with this specific ligand.

We recently obtained crystals of the  $\text{Zn}^{2+}$  complex  $[\text{Zn}(4\text{-bromocalcimycin})_2 \cdot \text{H}_2\text{O}]$ . X-Ray analysis of its structure revealed interesting features<sup>4</sup> (Fig. 4). Apart from the two highly different conformations, L1 and L2, in the benzoxazole region of the ligand in the dimeric association, which was marked, two other structural features emerged: (i) The 3-aminomethyl substituent was rotated out of the aromatic plane owing to the presence of the bulky bromine in the 4 position, and the existing intramolecular hydrogen bonding with the carboxylate shown for calcimycin<sup>6,7</sup> was suppressed. (ii) For

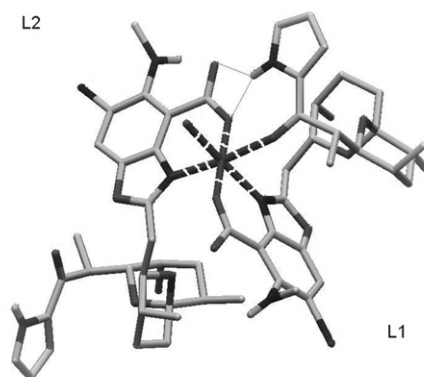


Fig. 4 X-Ray structure of the complex  $[\text{Zn}(4\text{-bromocalcimycin})_2 \cdot \text{H}_2\text{O}]$ .

the two ligands involved, the ketopyrrole arm adopted the preferred orientation already observed for calcimycin, corresponding to the A conformer previously discussed.

At this stage, we investigated the effect of the two conformational perturbations, introduced in the two liganding arms, on the formation of the supramolecular scaffold with divalent cations in solution. For a reliable comparison, calcimycin **1** was included in our measurements; the complex formation constants available for this ionophore under the same experimental conditions<sup>8,12</sup> were used to validate our method.

### Complex formation with divalent cations

For consistency with the previous work we carried out on calcimycin, we chose potentiometry in pure methanol for the characterisation of complexing abilities. The equilibria (1)–(3) were considered for the carboxylic ligands 1–3 (noted AH) and cations  $\text{M}^{2+}$ , with the corresponding thermodynamic constants,  $K_a^0$ ,  $\beta_1^0$ , and  $\beta_2^0$ :

$$\text{AH} \rightleftharpoons \text{A}^- + \text{H}^+ \quad K_a^0 = \frac{a(\text{A}^-, \text{H}^+)}{a(\text{AH})} \quad (1)$$

$$\text{M}^{2+} + 2\text{A}^- \rightleftharpoons \text{MA}^+ + \text{A}^- \quad \beta_1^0 = \frac{a(\text{MA}^+, \text{A}^-)}{a(\text{M}^{2+}, 2\text{A}^-)} \quad (2)$$

$$\text{M}^{2+} + 2\text{A}^- \rightleftharpoons \text{MA}_2 \quad \beta_2^0 = \frac{a(\text{MA}_2)}{a(\text{M}^{2+}, 2\text{A}^-)} \quad (3)$$

$K_a^0$  is related to the AH acid dissociation, while  $\beta_1^0$  and  $\beta_2^0$  characterise the formation of 1 : 1 and 1 : 2 complexes.

For a better comparison of the skeleton properties, we investigated the alkaline earth cation series, and we decided to add cations  $\text{Zn}^{2+}$  and  $\text{Mn}^{2+}$ , which are selectively transported by **3**.<sup>11</sup> For these two cations, we had shown previously<sup>12</sup> that it was necessary to introduce the formation of additional complexes with the methoxide ion  $\text{MeO}^-$  (noted  $\text{S}^-$ ), to obtain a close fit between experimental and simulated curves by least squares analysis. Equilibria (4)–(6) were thus taken into account:

$$\text{M}^{2+} + 2\text{S}^- \rightleftharpoons \text{MS}^+ + \text{S}^- \quad \beta_3^0 = \frac{a(\text{MS}^+, \text{S}^-)}{a(\text{M}^{2+}, 2\text{S}^-)} \quad (4)$$

$$\text{M}^{2+} + 2\text{S}^- \rightleftharpoons \text{MS}_2 \quad \beta_4^0 = \frac{a(\text{MS}_2)}{a(\text{M}^{2+}, 2\text{S}^-)} \quad (5)$$

$$\text{M}^{2+} + \text{A}^- + \text{S}^- \rightleftharpoons \text{MAS} \quad \beta_m^0 = \frac{a(\text{MAS})}{a(\text{M}^{2+}, \text{A}^-, \text{S}^-)} \quad (6)$$

Full details of the methodology are given in the Experimental.  $\text{p}K_a$  values of the ligands and  $\log \beta_1^0$  and  $\log \beta_2^0$  for the cations studied are given in Table 1. The parameters  $\sigma$  and  $\sigma_{Y/X}$  give

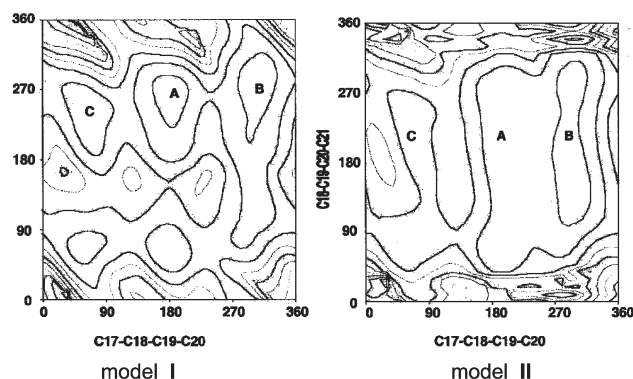


Fig. 3 Ramachandran plots.

**Table 1**  $\log\beta_1^0$  and  $\log\beta_2^0$  for ligands **1–3** (MeOH, 25 °C)

		$pK_a$	$Mg^{2+}$ (0.72 Å)		$Ca^{2+}$ (1.00 Å)		$Sr^{2+}$ (1.25 Å)		$Ba^{2+}$ (1.34 Å)		$Mn^{2+}$ (0.83 Å)		$Zn^{2+}$ (0.75 Å)	
			Expt	$\sigma$	Expt	$\sigma$	Expt	$\sigma$	Expt	$\sigma$	Expt	$\sigma$	Expt	$\sigma$
Calcimycin <b>1</b>	$\log\beta_1^0$	11.16	7.50	0.028	8.20	0.019	6.80	0.064	6.38	0.064	8.14	0.058	8.24	0.023
	$\log\beta_2^0$		16.2	0.045	16.5	0.046	14.4	0.018	12.5	0.098	17.8	0.094	18.34	0.014
	$\sigma_{Y/X}$		0.022		0.032		0.01							
19-Demethyl calcimycin <b>2</b>	$\log\beta_1^0$	11.78	6.5	0.044	7.25	0.008	4.89	0.004	5.55	0.009	6.20	0.007	8.20	0.008
	$\log\beta_2^0$		14.5	0.063	15.90	0.010	12.00	0.006	11.95	0.016	15.33	0.007	15.62	0.010
	$\sigma_{Y/X}$		0.028	0.030	0.010	0.007	0.030	0.032			0.038		0.040	
4-Bromo calcimycin <b>3</b>	$\log\beta_1^0$	9.04	6.0	0.031	6.08	0.008	5.47	0.006	5.03	0.004	6.42	0.009	6.72	0.009
	$\log\beta_2^0$		9.65	0.054	9.57	0.014	10.69	0.011	9.61	0.012	12.6	0.028	13.4	0.031
	$\sigma_{Y/X}$		0.054	0.014	0.007	0.005	0.048	0.027						

an indication of the measurement accuracy of the constants and the quality of the measurements, respectively.

In equilibrium (1), the acid dissociation of the carboxylic group proved different for each ligand. There was an increase of 0.6  $pK_a$  units for **2** compared with calcimycin, attributable to facilitated ketopyrrole arm mobility, the head-to-tail intramolecular chelation shown in the acid form<sup>8</sup> being disrupted. For **3**, both the steric and substituent effects of the bromine are responsible for a large  $pK_a$  decrease of two orders of magnitude.

In the  $MA^+$  formation, corresponding to equilibrium (2),  $\log\beta_1^0$  values range between 5 and 8, which indicates a marked stability of the 1 : 1 species. The strong ability to form  $MA_2$  neutral complexes following equilibrium (3), with what we previously called a cooperative effect,<sup>13</sup> is preserved if we compare  $\log\beta_2^0$  with  $\log\beta_1^0$  in each  $M^{2+}$ –ligand couple for calcimycin **1** and its demethyl analogue **2**. On the other hand, for 4-bromocalcimycin (**3**) the 1 : 2 association is strongly destabilised, especially for the alkaline earth series. This explains the wide range in  $\log\beta_2^0$  values, between 9.5 to 18, shown in Table 1 for the three ligands.

## Discussion

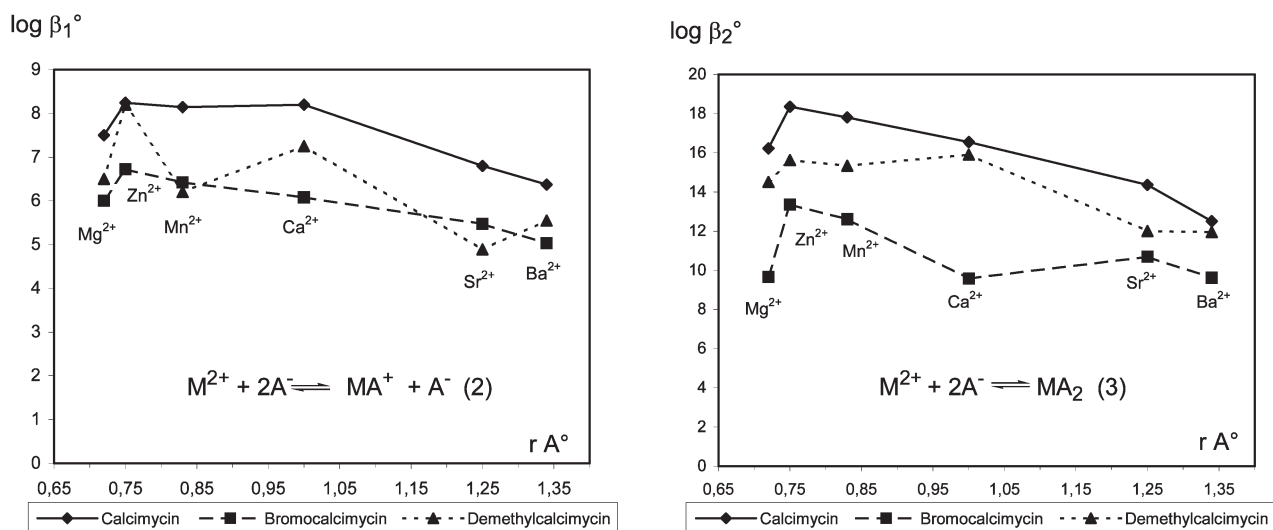
A plot of  $\log\beta^0$  versus ionic radii<sup>14</sup> (Fig. 5) helps to analyse the results. All the cations are included in the plots, but it must be kept in mind that the coordinating properties of alkaline earth cations, with their rare gas structures, are different from those of  $Zn^{2+}$  ( $[Ar]3d^54s^0$ ) and  $Mn^{2+}$  ( $[Ar]3d^54s^0$ ).

Calcimycin is definitely the best liganding system with the preference order:  $Zn^{2+} > Mn^{2+} \geq Ca^{2+}$  (0.75 to 1.0 Å). Values

are in close agreement with the previous values obtained under the same experimental conditions.<sup>8,12</sup> There was not a gap in favour of  $Mn^{2+}$ ,  $Zn^{2+}$  compared with the alkaline earth cations, very likely because compounds **1**, **2** and **3** are highly dissymmetrical ligands with binding sites of different electronic properties: COO<sup>−</sup>, N-benzoxazole, C=O pyrrole. Further, they are distributed in a chiral chain with preferential conformations. So, these binding sites are not free in comparison with small independent ligands. In Table 2 are given the calculated  $\delta\log\beta^0$  shifts for the two analogues using the corresponding  $\log\beta^0$  of calcimycin as references.

For the 1 : 1 association, we show for the first time that the removal of 19-CH<sub>3</sub>(S) in **2** systematically weakens complex formation, except for  $Zn^{2+}$ , with  $\delta\log\beta_1^0$  ranging from 0.73 to 1.94. Kinetics studies in methanol have shown that equilibrium (2) is the rate-limiting step in the neutral complex formation.<sup>8,13</sup> Our new experiments emphasise the role of the ketopyrrole arm conformation in this crucial step. Interestingly, the 4-bromo substitution made on the benzoxazole arm in **3** also results in a decrease in the 1 : 1 complex formation, characterised by values of  $\delta\log\beta_1^0$  ranging from 1.25 to 2.12.

Structurally, the transient 1 : 1 association for calcimycin has never been studied in solution by NMR. However, electronic spectra corresponding to the 1 : 1 and 1 : 2 species had been calculated from the spectrophotometric measurements for the calcium and magnesium complexes.<sup>8</sup> Similar  $\lambda_{max}$  were obtained while the  $\epsilon$  for  $MA_2$  was about twice that of  $MA^+$ . This suggested an identical cation–ligand association in both cases and brings us to the issue of a putative tripod coordination as shown in Fig. 6. In this schematic representation, the divalent cation is still partially solvated. Interestingly, a quite

**Fig. 5** Equilibrium constants  $\log\beta_1^0$  and  $\log\beta_2^0$  versus ionic radii (in Å).

**Table 2**  $\delta\log\beta^0$  values for **2** and **3** from ref. 1

	Mg <sup>2+</sup>	Ca <sup>2+</sup>	Sr <sup>2+</sup>	Ba <sup>2+</sup>	Mn <sup>2+</sup>	Zn <sup>2+</sup>
$\delta\log\beta_1^0$ <b>1–2</b>	1.0	0.95	1.9	0.73	1.94	0.04
$\delta\log\beta_2^0$ <b>1–2</b>	1.7	0.6	2.4	0.55	2.47	2.72
$\delta\log\beta_1^0$ <b>1–3</b>	1.5	2.12	1.33	1.25	1.72	1.52
$\delta\log\beta_2^0$ <b>1–3</b>	6.55	6.93	3.71	2.89	5.2	4.94

similar 1 : 1 structure has been described by crystallography for X-14885A,<sup>15</sup> a closely related calcimycin analogue, with the monovalent cation Na<sup>+</sup>. For this 1 : 1 complex our results show that a methyl group in the 19 position adds stability to the scaffold, possibly related to the preferred A conformation adopted by the ketopyrrole arm. At the other end of the claw, planarity of the whole benzoxazole moiety is required for complex formation, since removal of the NH(CH<sub>3</sub>)...COO<sup>−</sup> hydrogen bond (see Fig. 4) also decreases the association constants.

As regards the 1 : 2 association, there is a drastic destabilisation of MA<sub>2</sub> formation with compound **3**, which is specifically important for Ca<sup>2+</sup>. The selectivity Zn<sup>2+</sup> > Mn<sup>2+</sup> is retained (Fig. 5). All the formation constants are greatly lowered compared with calcimycin, with a drop of stability as measured by  $\delta\log\beta^0$  ranging from 2.89 to 6.93. These results are consistent with the transport experiments performed in phospholipid vesicles and the discussion presented,<sup>11</sup> especially as the authors concluded that 4-bromocalcimycin is a low-activity ionophore for calcium. The transport selectivity in favour of Zn<sup>2+</sup> over Mn<sup>2+</sup> can be explained by the partial conservation of 1 : 1 and 1 : 2 complex stabilities for these cations. Disruptions introduced by the bromine substituent in compound **3** definitely deorganise the molecular scaffold. This is illustrated by the dimeric Zn<sup>2+</sup> structure we have studied<sup>4</sup> (Fig. 4) in which the ligand was unable to achieve a complete coordination sphere by its own coordinating sites. If the solid state structure reflects the situation in solution, then the decrease in  $\beta_2^0$  is also due to the loss of one of the pyrrole NH bonds (L2) to the carboxyl oxygen of the other ionophore (L1), which was observed for the calcimycin-M<sup>2+</sup> solid state structures.<sup>6,7</sup>

Interestingly, the destabilisation process observed for 19-demethylcalcimycin **2** in equilibrium (2) is not intensified for MA<sub>2</sub> formation, particularly for Mg<sup>2+</sup>, Ca<sup>2+</sup> and Ba<sup>2+</sup>, since  $\delta\log\beta_2^0$  values range between 0.6 to 1.7. Decrease in stability is more pronounced for other cations, and in the case of Zn<sup>2+</sup> where  $\log\beta_1^0$  is about the same as for the 19-demethyl analogue compared to calcimycin, the difference is 2.7 for  $\delta\log\beta_2^0$ . As stated above, the structure of the neutral association complex is well-documented for calcimycin.<sup>6–8</sup> From these

results it appears that the increased mobility of the ketopyrrole arm in compound **2** does not notably prevent the formation of this very stable supramolecular structure for calcium, which is the main target in biological studies.

## Experimental

### Ligands

Calcimycin or A23187 (**1**) was a laboratory stock sample isolated from the strain *Streptomyces chartreusis* NRRL 3882.<sup>8</sup> We prepared 19-demethylcalcimycin (**2**) by hemisynthesis from the natural metabolite.<sup>3</sup> 4-Bromocalcimycin (**3**) was obtained by the described method.<sup>9</sup> <sup>1</sup>H NMR (CDCl<sub>3</sub>, 400 MHz), <sup>13</sup>C NMR (CDCl<sub>3</sub>, 100 MHz) and high-resolution MS were used to confirm the correct monobromination reaction on the magnesium salt of calcimycin.

### Molecular modelling

MacroModel<sup>®</sup> Program was the commercial version 7.0. Interatomic distances and angles were those of ref. 6. As we were interested here in the ketopyrrole arm mobility, with or without a 19-Me group, we studied the simplified model shown in Fig. 1 to reduce the calculation time. The OPLS-AA force field was used with conjugate gradient energy minimisation to obtain the relative energy *versus* torsion angle plots shown in Fig. 2 and the Ramachandran plots in Fig. 3.

### Potentiometric measurements

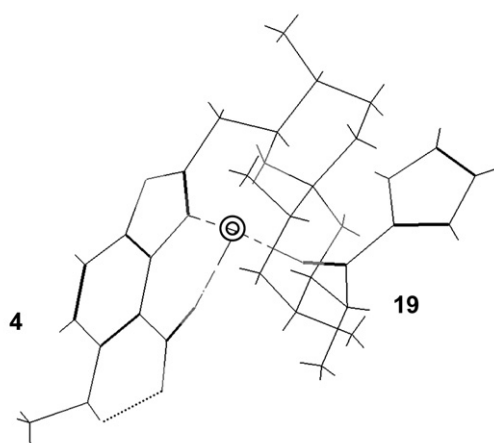
**Principle.** Acid-base titration of a methanol solution was performed for each ligand using tetrabutylammonium methoxide (tBu<sub>4</sub>N<sup>+</sup>MeO<sup>−</sup>) in methanol, in the presence or absence of a metal salt.<sup>8,12</sup> This base was used for its bulky cation, which cannot form association complexes with the ligands. Cation complexation increased the ligand acidity, so the pH curves were lowered. This modification enabled us to determine the thermodynamic constants for equilibria (1)–(6). All experiments were carried out at 25 °C.

**Products.** Anhydrous methanol (Merck, water-free) containing less than 0.01% of water was chosen as solvent. We used as the titrating base a freshly prepared<sup>16</sup> tBu<sub>4</sub>N<sup>+</sup>MeO<sup>−</sup> solution in methanol† instead of tBu<sub>4</sub>N<sup>+</sup>OH<sup>−</sup> in water, which was often found to be carbonated. Thus, the medium was almost free of OH<sup>−</sup>, which was liable to compete with MeO<sup>−</sup> in the formation of mixed complexes (equilibria (4)–(6)).

Perchlorates (Strem) were used for the alkaline earth, manganese and zinc cations. These salts are completely dissociated in methanol. As they are hygroscopic, they were stored in a vacuum (10<sup>−3</sup> atm) and titrated<sup>17</sup> just before the potentiometric measurements, using 0.100 mol·L<sup>−1</sup> aqueous Titriplex<sup>®</sup> III solution and a buffer indicator tablet (Merck) containing eriochrom black T. Salt solutions in methanol were made up simultaneously to prevent an increase in their water content.

Solutions were prepared by weighting all the components.

**Electrodes.** Potentiometric measurements were performed using a calomel reference electrode in methanol, with a bridge junction filled with a 0.1 mol·L<sup>−1</sup> tBu<sub>4</sub>N<sup>+</sup>ClO<sub>4</sub><sup>−</sup> solution in

**Fig. 6** Putative structure of the 1 : 1 complex.

† To a solution of 11.1 g (30 mmol) of tBu<sub>4</sub>N<sup>+</sup>I<sup>−</sup> in 100 mL of anhydrous methanol was added, at 0 °C under argon pressure and in the dark, 8.0 g (32.3 mmol, 1.1 equiv.) of silver(I) oxide. The solution was stirred 2.5 h before filtration. The precipitate was washed with small volumes of anhydrous methanol. The filtrate was then quickly titrated with a 0.100 mol·L<sup>−1</sup> solution of hydrochloric acid in the presence of 1 or 2 drops of phenolphthalein. A more accurate titration is obtained by the potentiometric technique of a diluted alkaline solution (1/100) using a 0.010 mol·L<sup>−1</sup> solution of hydrochloric acid.



methanol and a  $\text{H}^+$  glass electrode (Orion 91-01A) as the indicator electrode. This system enabled us to follow the e.m.f. of the cell containing the ligand solution in the presence or absence of a metal salt.

The following experimental conditions were used: 25 mL of the acidic solution ( $C_{\text{AH}}^0 \cong 6 \times 10^{-4} \text{ mol}\cdot\text{L}^{-1}$ ) was neutralised by 30 successive additions of approximately 0.2 mL of the basic solution ( $C_{\text{M}}^0 \cong 5 \times 10^{-3} \text{ mol}\cdot\text{L}^{-1}$ ), delivered by a calibrated automatic burette, when the salt concentration was  $C_{\text{M}}^0 \cong 3 \times 10^{-4} \text{ mol}\cdot\text{L}^{-1}$ .

The De Ligny salicylate buffer<sup>18</sup> in methanol was used to convert e.m.f. to pH scale for this solvent. Plots of pH vs.  $V_{\text{b}}$  (added basic solution) were used to obtain the thermodynamic constants.

**Data processing.** Curves were processed by the least-squares method to obtain  $\beta_1^0$  and  $\beta_2^0$ , by taking account of the activity coefficients (Debye–Hückel), corresponding to eqns. (1)–(6).

As we were working in diluted medium, our measurements were disturbed by the presence of a monoacid impurity ( $C \cong 10^{-4} \text{ mol}\cdot\text{L}^{-1}$ ,  $\text{p}K_{\text{a}} = 11.2 \pm 0.1$ ), which may have been either dissolved  $\text{CO}_2$  or an acid residue specific to the solvent. This impurity was not eliminated in the experiments. Accordingly, we made a numerical correction: the least-squares program was modified by adding to the chemical model the dissociation equilibrium of this acidic impurity. This introduced a new unknown factor: the impurity concentration.

Equilibrium constants  $\beta_3^0$  and  $\beta_4^0$  were independently determined ( $\text{Zn}^{2+}$ :  $\log\beta_3^0 = 7.1$ ,  $\log\beta_4^0 = 15.2$ ;  $\text{Mn}^{2+}$ :  $\log\beta_3^0 = 6.5$ ,  $\log\beta_4^0 = 13.7$ ); the values obtained were in agreement with previous ones.<sup>12</sup> For the processing, fixed values for  $K_{\text{a}}^0$ ,  $\beta_3^0$  and  $\beta_4^0$  were used. Equilibrium constants  $\beta_1^0$ ,  $\beta_2^0$  and  $\beta_{\text{m}}^0$  were subjected to refinement.

**Resolution.** A grid method allowed us to visualise the form of the function:  $\text{fmc} = \sum (\text{pH}_{\text{exp.}} - \text{pH}_{\text{calc.}})^2$  and to approach the order of magnitude of the parameters sought, near the minimum of fmc. The linearisation method then afforded the matrix, which associated with  $\sigma_{Y/X}$ , gave the standard deviations corresponding to each constant.

$\sigma_{Y/X} = (\text{fmc}/N)^{1/2}$ , where  $N$  is the number of experimental points, is a good indicator of the quality of the measurements when the chosen model is correct. It must be remembered that it contains the experimental errors and possibly the error due to the choice of the chemical model.

## Conclusion

The calcium carrier property of calcimycin (A23187) has been attested to by thousands of experiments conducted in the biological domain since its discovery. The use of this chemical entity has made a huge contribution to the study of the “calcium-life and death signal”.<sup>19</sup> What makes this open-chain bacterial metabolite so efficient in the transport of calcium through membranes? Much work has been conducted to address this question, one of the best model system used for this purpose probably being phospholipid vesicles.<sup>5</sup> Our bioorganic approach *via* closely related analogues, coupled with complexation measurements in solution, aim to study the molecular properties of the ligand. If we focus on calcium, from the study of 19(S)-CH<sub>3</sub>, coming from a propionate precursor in the biosynthesis,<sup>20</sup> is mainly to stabilise the 1 : 1 transient complex formation. On the other hand, 4-H substitution by the bulky bromine substituent in derivative **3** destabilises the 1 : 1 complex and almost prevents 1 : 2 complex formation for the alkaline earth cations (especially  $\text{Mg}^{2+}$  and  $\text{Ca}^{2+}$ ). For  $\text{Zn}^{2+}$  and  $\text{Mn}^{2+}$ ,  $\log\beta_1^0$ ,  $\log\beta_2^0$  and the ratio  $\log\beta_2^0/\log\beta_1^0$  are substantial and consistent with ionophore properties.<sup>11</sup>

From previous<sup>8,13</sup> and present results we can summarise what emerges concerning the molecular properties of calcimycin as follows: (i) The benzoxazole arm supplies two coordinating sites (O-carboxylate and N-oxazole) that must be kept in a plane for maximum stability of the 1 : 1 and 1 : 2 scaffold; this is accomplished by the hydrogen bond network in the natural structure (see Fig. 6). Also, this moiety can find an appropriate orientation towards the water phase at the water–membrane interface to interact with  $\text{Ca}^{2+}$  ( $\text{H}^+ \leftrightarrow \text{Ca}^{2+}$  exchange), due to its conformational mobility.<sup>8</sup> (ii) The ketopyrrole arm brings one coordinating  $\text{C}_{20}=\text{O}$  site positioned to achieve 1 : 1 complex formation, owing to the preferential conformation of the C18–C19–C20 part. Clearly, the natural structure attains perfection for the 1 : 1 step, but replacement of 19(S)-CH<sub>3</sub> by  $-\text{H}$  does not have a drastic effect. (iii) The spiroketal structure, which is present in a very great number of natural compounds, is involved in the chemical architecture by bringing a chiral helical support to the coordinating arms branched in the 10*eq* and 18*eq* positions. The 1 : 2 complex units two ligands of the same helicity; this also likely contributes to the stability of the neutral scaffold.

These findings may thus help to design new biomimetic systems displaying efficient ionophore properties for divalent cations.

## Acknowledgements

This work was supported by the C.N.R.S. and the Ministère de l'Éducation Nationale, de la Recherche et de la Technologie (S.V. benefited from a “M.E.N.R.T. thesis grant”).

## References

- 1 M. O. Chaney, P. V. Demarco, N. D. Jones and J. L. Occolowitz, *J. Am. Chem. Soc.*, 1974, **96**, 1932.
- 2 See, for instance: G. A. Woolley, D. R. Pfeiffer and C. M. Deber, *Methods in Neurosciences*, Academic Press, Orlando, 1995, vol. 27, pp. 52–68.
- 3 S. Vila, I. Canet, J. Guyot and G. Jeminet, *J. Chem. Res. (S)*, 2002, 634.
- 4 S. Vila, I. Canet, J. Guyot, G. Jeminet and L. Toupet, *Chem. Commun.*, 2003, 516.
- 5 W. L. Erdahl, C. J. Chapman, R. W. Taylor and D. R. Pfeiffer, *Biophys. J.*, 1994, **66**, 1678.
- 6 G. D. Smith and W. L. Duax, *J. Am. Chem. Soc.*, 1976, **98**, 1578.
- 7 M. Alléaume and Y. Barrans, *Can. J. Chem.*, 1985, **63**, 3482.
- 8 A. M. Albrecht-Gary, S. Blanc-Parasote, D. W. Boyd, G. Dauphin, G. Jeminet, J. Juillard and C. Tissier, *J. Am. Chem. Soc.*, 1989, **111**, 8598.
- 9 M. Debono, R. M. Molloy, D. E. Dorman, J. W. Paschal, D. F. Babcock, F. Donner, C. M. Deber and D. R. Pfeiffer, *Biochemistry*, 1981, **20**, 6865.
- 10 C. M. Deber, J. T. Kun, E. Mack and S. Grinstein, *Anal. Biochem.*, 1985, **146**, 349.
- 11 W. L. Erdahl, C. J. Chapman, E. Wang, R. W. Taylor and D. R. Pfeiffer, *Biochemistry*, 1996, **35**, 13 817.
- 12 M. Tissier, A. Ouahabi, G. Jeminet and J. Juillard, *J. Chim. Phys.*, 1993, **90**, 595.
- 13 A. M. Albrecht-Gary, S. Blanc, L. David and G. Jeminet, *Inorg. Chem.*, 1994, **33**, 518.
- 14 Y. Marcus, *Chem. Rev.*, 1988, **88**, 1475.
- 15 J. W. Westley, C. M. Liu, J. F. Blount, L. M. Selo, N. Troupe and P. A. Miller, *J. Antibiot.*, 1983, **36**, 1275.
- 16 M. R. Cundiff and P. C. Markunas, *Anal. Chem.*, 1962, **34**, 584.
- 17 *Méthode d'Analyses Complexométriques par les Titriplex®*, Merck Co., Darmstadt, 3rd edn.
- 18 C. L. de Ligny, P. F. M. Luykx, M. Rehbach and A. A. Weineke, *Rec. Trav. Chim. Pays-Bas*, 1960, **79**, 699.
- 19 M. J. Berridge, M. D. Bootman and P. Lipp, *Nature (London)*, 1998, **395**, 645.
- 20 M. J. Zmijewski, Jr., R. Wong, J. W. Paschal and D. E. Dorman, *Tetrahedron*, 1983, **39**, 1255.